Supplementary Information: An evaluation of airborne mass balance and tracer correlation approaches to estimate site-level CH_4 emissions from LNG facilities using CO_2 as a tracer of opportunity

Mark F. Lunt[1], Stephen J. Harris[2,3], Jorg Hacker[4,5], Ian Joynes[6], Tim Robertson[7], Simon Thompson[7], James L. France[8,9]

[1]Environmental Defense Fund, Perth, WA, Australia
[2]UNEP's International Methane Emissions Observatory (IMEO), Paris, France
[3]School of Biological, Earth and Environmental Sciences, University of New South Wales, Sydney, NSW, Australia
[4]Airborne Research Australia, Parafield, SA, Australia
[5]College of Science and Engineering, Flinders University, Adelaide, SA, Australia
[6]Woodside Energy Limited, Perth, WA, Australia
[7]Chevron Australia Pty Ltd, Perth, WA, Australia.
[8]Environmental Defense Fund Europe, Brussels, Belgium
[9]Earth Sciences Dept, Royal Holloway University of London, Egham, UK

Contents

S1 Aircraft description

The Diamond aircraft HK36TTC-ECO Dimona operated by Airborne Research Australia has a cruising speed of 30-55 m s^{-1}, allowing relatively high spatial resolution of atmospheric measurements. It has a flight endurance of 5-6 hours enabling multiple passes of measurement targets per flight, even with substantial transfer distance from the nearest useable airport. The Dimona's ROTAX engine uses premium unleaded petrol which helps to limit the risk of cross-contamination of samples. The Dimona can operate between 50 m (with special clearance) and 6000 m altitude, although the upper limit was not

approached in this study. Maximum take-off weight is 930 kg, allowing around 150 kg payload for scientific instruments. The electrical supply available to scientific instrumentation is 100 A at 24 V.

S2 Flight planning

For the mass balance calculations, downwind transects were flown to generate a single screen or curtain. For most flights, a mission scientist was also the pilot of the research aircraft to ensure optimum flight patterns for emissions quantifications with respect to direction, vertical spacing and distance from the source(s). Decisions on flight paths were made in real time based on the onboard display of the CH_4, CO_2 and other tracers. These included real-time measured wind speed and direction in addition to visual clues from the outside of the aircraft such as tankers being loaded or flaring taking place. On days when the mission scientist was not piloting the Dimona aircraft, the mission scientist monitored most parameters remotely via an AnyDesk remote desktop connection and instructed the pilot regarding flight strategy in real-time.

As far as possible, transects were flown perpendicular to the mean wind direction. Occasionally, due to difference in forecast and observed winds or wind direction changes during the flight, the curtain angle deviated from perpendicular by up to 33°. The angle difference between aircraft heading and flux through a perpendicular plane is accounted for by the perpendicular wind speed term, $v_{\perp i}$, in Eq. 1 of the main text. The impact of curtain heading on the comparison between mass balance CO_2 estimates and operator CO_2 reporting is shown in Fig. S1. This shows no discernible relationship between the two.

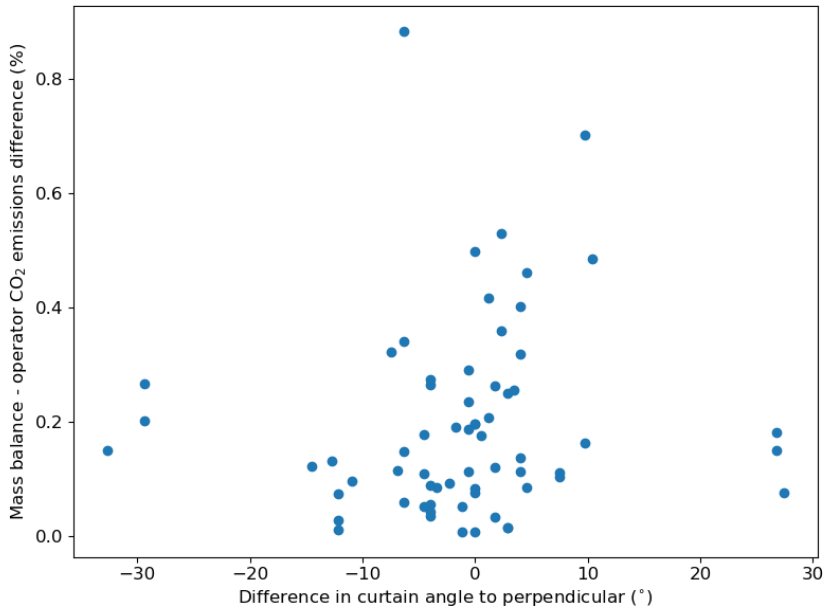

Figure S1: Impact of curtain angle on difference between mass balance and operator estimates.

S3 Additional (non-quantified) curtains

Figure 4 in the main text shows the impact of wind speed on the difference between CO2 emissions estimated via the mass balance approach compared to the operator's estimates. The lowest mean wind speed was 3.0 m s^{-1}. However, there was an additional flight day where the data from two curtains were excluded from our analysis due to a clear violation of the mass balance assumptions. The mean wind speeds for the respective curtains were 1.8 and 2.0 m s^{-1}.

An example of one of these curtains is shown in Figure S2, which shows the CH_4 and CO_2 enhancements, as well as the wind speeds and direction along each transect. For this curtain, the most extensive CH_4 and CO_2 enhancements were observed at altitudes above 600 m. In this case, wind directions were not consistently from the direction of the emitting site, and the assumptions of constant transport applied in the mass balance equation did not apply. Below 400 m, the wind speed was 3.3 m s^{-1}, and the median wind direction was 25°, consistent with the curtain position to the south-west of the site. The average CO_2 enhancement in the plume was 0.7 ppm. Above 400 m, the wind shifted such that the speed was 1 m s^{-1}, while the median wind direction shifted from 25° to 195° degrees, and the mean CO_2 enhancement was larger at 1.3 ppm, indicating potential recirculation of the downwind signal. There was no known significant source to the south that could have generated these observed enhancements. Since the observed conditions were not suitable for a mass balance quantification using the single screen approach, we omitted the curtains from this date in our analysis. A naïve attempt at a mass balance calculation from this curtain resulted in a CO_2 emission rate that was only 10% of the average of all other curtains. This example shows that the mass balance quantification performance may degrade significantly beyond that shown in Figure 4 of the main text under low wind speed or variable wind conditions.

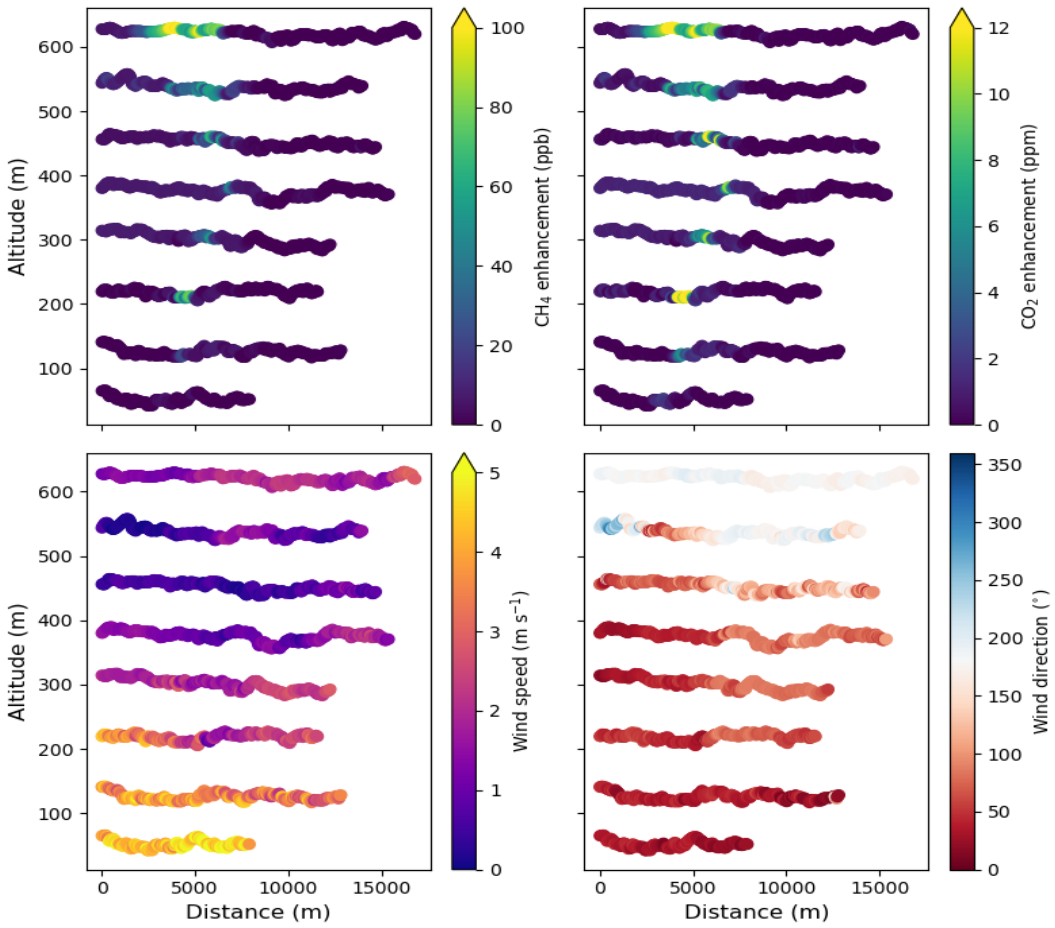

Figure S2: Example downwind curtain data excluded from mass balance calculations. (a) CH_4 enhancements above background along each transect which peak above 600 m. (b) CO_2 enhancements above background which show a similar pattern. (c) Wind speed along each transect which change from around 5 m s^{-1} below 100 m to less than 1 m s^{-1} around 500 m. (d) Wind direction which shifted from a NE direction to S above 500 m. The LNG facility was to the NE of the downwind curtains.

S4 Sampling density

A sensitivity test was conducted to determine the impact of the vertical spacing of transects on the individual curtain quantifications. The results presented in the main text used an average vertical spacing between transects of 75 m. In the sensitivity test, this was increased to 150 m, by omitting every second transect from each of the 83 mass balance curtains used in the analysis of the main text. The first transect to be omitted was always the lowest altitude transect flown. This increased the vertical distance of the surface extrapolation by 75 m on average. As a result, the proportion of the total integrated mass flux estimated by the surface extrapolation increased. If the surface extrapolation term caused significant error in the total curtain quantification we would expect to observe this in the comparison to operator estimates.

Figure S3 shows a comparison of the mass balance - operator differences when using the full density curtains versus the half density curtains. The relative mean absolute error of the half density curtains was 25%, compared to 20% when using all transects in each curtain. Mean biases relative to the operator estimates remained similar between the two sets of results at 3% for full density curtains and 5% for the half density curtains. The results suggest a limited impact of both the vertical sampling density and the height of the lowest transect on the emission estimates.

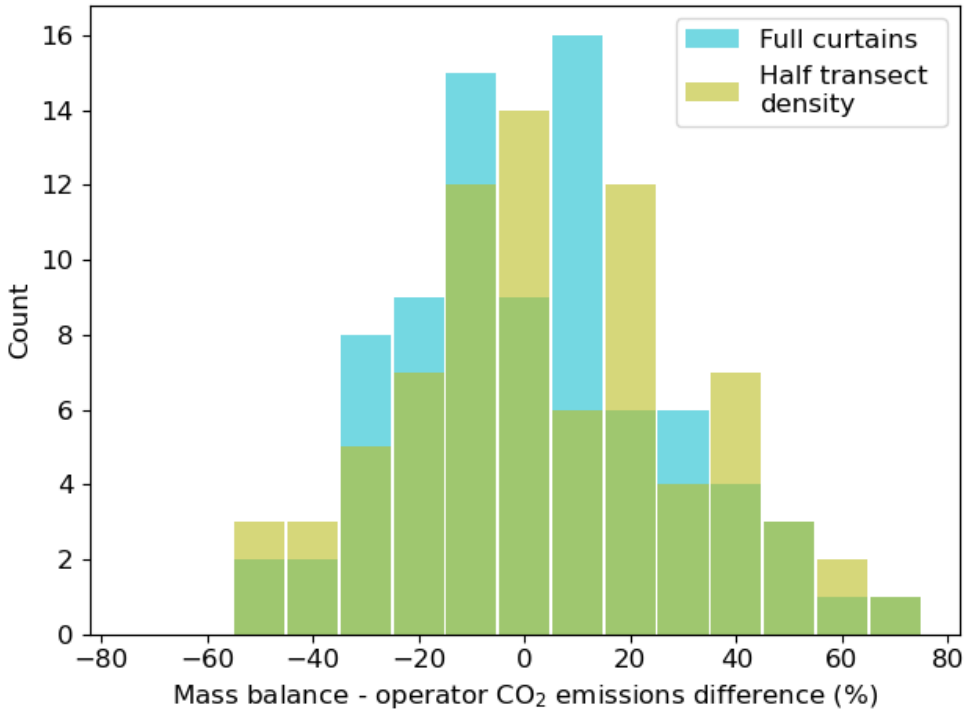

Figure S3: Histograms showing a comparison of the distribution of relative differences between mass balance and operator estimates across all sites when using all transects versus only half the available transects for each curtain.

S5 Curtain level correlations vs transect correlations

Figure 6 of the main text shows scatter plots of CO_2 and CH_4 mole fraction enhancements measured on different days at one of the sites. Whilst the ordinary least squares best fit lines are relatively consistent across the different days, the coefficients of determination are as low as 0.43, indicating that at the curtain level (equivalent to whole site) less than 50% of the variability in CH_4 enhancements can be explained by CO_2.

Figure S4 and S5 show plots of the distribution of the coefficients of determination for individual transects as well as the OLS ratios per transect. Figure S4 shows that the majority of CH_4 variability for individual transects can be explained by CO_2, with more than 50% of transects having coefficients of determination greater than 0.8 for each curtain.

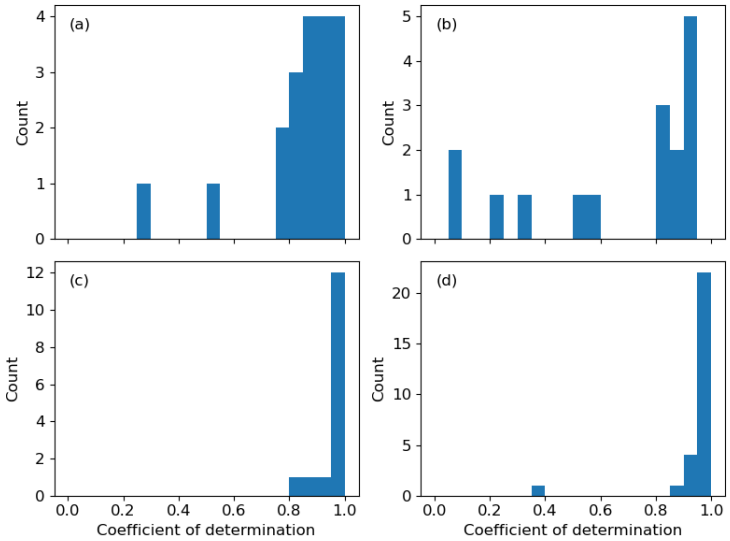

Figure S4: Distribution of the coefficients of determination of individual transects between CH_4 and CO_2 mole fractions for each of the 4 days shown in Figure 6 in the main text. Each panel (a)-(d) represents a different day of measurements at the same LNG site. The overall coefficients of determination for all data were: (a) 0.77, (b) 0.49, (c) 0.78, (d) 0.96.

The overall site-level correlations are smaller because the ratios of those individual transects are not consistent, as shown in Figure S5. In panels (a)-(c) there are a range of transect ratios. A consistent mean site-level ratio will only eventuate through even sampling of each of these different ratios across the different transects. The transect ratios on the fourth day in panel (d) are much more consistent with the site-level gradients. This is likely because these measurements were performed further downwind (8 km) and the individual transects are more representative of site-level emission ratios than source level.

The results imply that the individual transects may be more representative of source-level correlations or affected by different vertical transport of CH_4 and CO_2 due to different release temperatures rather than site-level averages. Whilst the site-level correlations may appear relatively weak, these are underpinned by relatively strong (>0.8) coefficients of determination along individual transects. Consistent site-level ratios eventuate from averaging of the relatively highly correlated transect ratios.

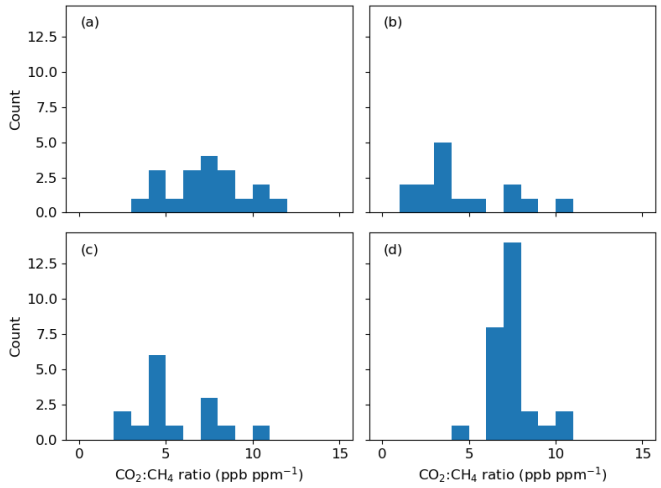

Figure S5: Distribution of the CH_4:CO_2 ratios for individual transects for each of the 4 days shown in Figure 6 of the main text. Each panel (a)-(d) represents a different day of measurements at the same LNG site. The overall ratios of all data on each day were: (a) 7.2, (b) 7.1, (c) 6.6 and (d) 7.2 ppb ppm^{-1}.

S6 Temperature dependence of ratios

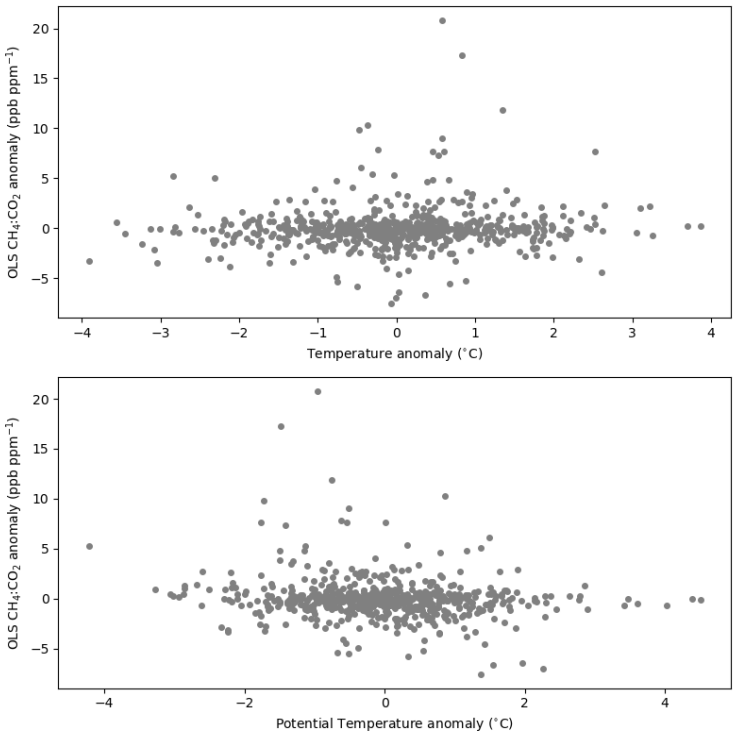

Figure S6: Ratios as a function of (a) temperature anomalies and (b) potential temperature anomalies. Anomalies are relative to the daily mean. Any impacts of different temperature of gas emissions at source on the CH_4:CO_2 ratios are not observable at the point of measurement.

S7 Ratio calculations with and without background subtraction

The ratios were calculated based on the mole fraction enhancements above background levels which first had to be determined following the process outlined in Section 2.2. Here, we examine the impact on CH_4 emissions estimated via the CO_2 tracer correlation approach if the background component is not removed from the raw measurement data. CH_4:CO_2 ratios were estimated using the same random sampling of 200 data points from different altitudes, with 200 different random sets of 200 observations used on each date to build up the distribution. The only difference to the results in the main text was to use the raw mole fractions rather than the mole fraction enhancements.

Figure S7 is the same as Fig. 9 of the main text but with an additional violin added to represent the distribution when using the raw mole fraction data with no background subtraction. The background levels are accounted for through the calculation of the intercept in the OLS regression, albeit this intercept covers data measured at all altitudes and different times. In this case of using the raw mole fractions, the mean estimate remains within 5% of the integrated plume ratios and the median is equivalent to the mass balance ratio. The distribution is wider, with a 27% standard deviation with some probability of low or even negative emissions. This contrasts with the result from the main text where the standard deviation of the distribution is 15% when background levels are subtracted. Negative values are only likely when the enhancements of either gas are smaller than the variation in background across altitudes or smaller than background variations over the course of a few hours.

The results show the value of properly accounting for the background contribution when incorporating data from different altitudes to calculate the CH_4:CO_2 ratio to minimize the uncertainty on the emission estimates. Nevertheless, the overall distribution provides comparable estimates of the CH_4 emissions magnitude to the other approaches, when no background subtraction is performed prior to calculating the CH_4:CO_2 ratios.

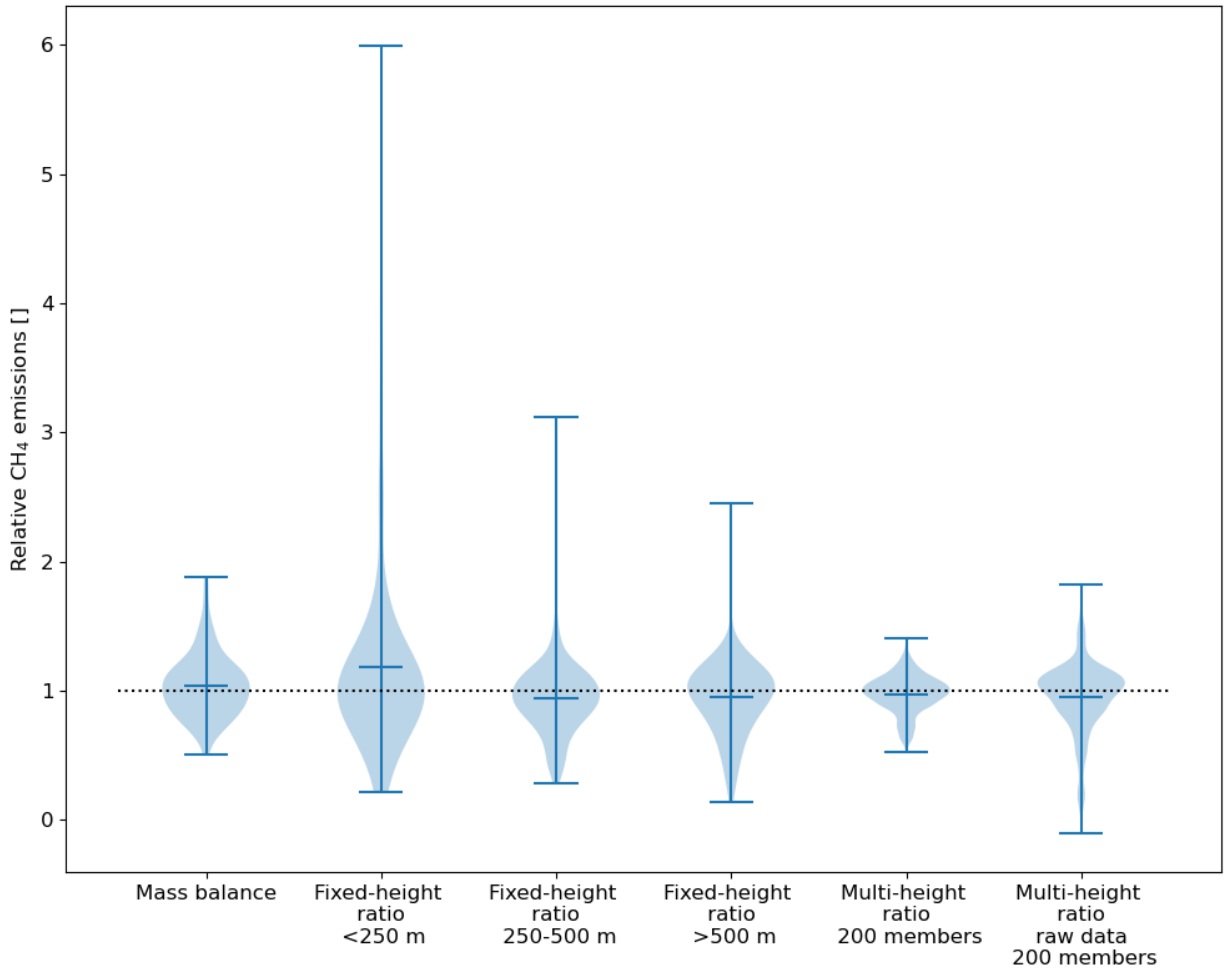

Figure S7: Same as Fig. 9 from the main text but with an additional violin based on using raw mole fractions that include the background contribution.

190